

THE ORIGIN OF COSMIC RAYS - A 96-YEAR-OLD PUZZLE SOLVED?

ARNON DAR

Department of Physics and Space Research Institute,
Technion, Haifa 32000, Israel

Abstract

There is mounting evidence that long duration gamma ray bursts (GRBs) are produced by ultra-relativistic jets of ordinary matter which are ejected in core collapse supernova (SN) explosions. Such jets are extremely efficient cosmic ray (CR) accelerators which can accelerate the swept up ambient particles on their way to the highest observed CR energies. The bulk of the jet kinetic energy is used to accelerate CRs while only a tiny fraction is used to produce the GRB and its afterglow. Here we use the remarkably successful cannonball (CB) model of GRBs to show that the bipolar jets from SN explosions, which produce GRBs most of which are not beamed towards Earth, can be the main origin of cosmic rays at all energies. The model explains very simply the elemental composition of CRs and their observed spectra at all energies. In particular it explains the origin of the CR knees and ankle. Above the CR ankle, the Galactic magnetic fields can no longer delay the free escape of ultra-high energies CRs (UHECR) from the Galaxy, and the CRs from the intergalactic medium (IGM), which were injected there by SN jets from all the galaxies and isotropized there by the IGM magnetic fields, dominate the Galactic CR spectrum. A Greisen-Zatsepin-Kuzmin (GZK) cutoff due to the interaction of UHECRs with the microwave background radiation is expected. The CR nuclei which diffuse out of galaxies, or are directly deposited in the IGM by the relativistic SN jets, may be the origin of the IGM magnetic fields. Inverse Compton scattering of the cosmic microwave background radiation (MBR) by the CR electrons in the IGM produces the diffuse extragalactic gamma-ray background radiation (GBR).

1 Introduction

Cosmic rays (CRs) were discovered by Victor Hess in 1912. Today, 92 years later, their origin is still unknown. CRs have been studied in experiments above the atmosphere, in the atmosphere, on the ground, underground and in space. Their energies cover an enormous range, from sub GeV to more than a few 10^{11} GeV, over which their differential flux decreases by roughly 33 orders of magnitude. Any successful theory of the origin of CRs must explain their main observed properties near Earth (for recent reviews see, e.g. Biermann & Sigl 2001; Watson 2001,2003; Olinto 2004; Cronin 2004) – **The CR energy spectrum** shown in Fig.1 has been measured up to hundreds of EeV. It can be approximated by a broken power-law, $dn/dE \sim E^{-p}$, with a series of breaks near 3 PeV known as ‘the knee’, a second ‘knee’ near 200 PeV and an ‘ankle’ near 4 EeV. The power-law index changes from $p \sim 2.67$ below the knee to $p \sim 3.05$ above it and steepens to $p \sim 3.2$ at the second knee. At the ankle, the spectral index changes to $p \sim 2.7$. The spectral behaviour above 50 EeV is still debated (see, e.g. Olinto 2004; Cronin 2004).

The CR elemental composition is known well only from direct measurements on board satellites, which run out of statistics well below the knee energy. The measured composition of high energy CRs is highly enriched in elements heavier than hydrogen relative to that of the solar system, as shown in Table I for TeV CRs. The enrichment increases with atomic number and with CR energy almost up to the second knee, beyond which it appears to decline (e.g., Kampert et al. 2004; Hoerandel 2004). It is still debated at energies above the ankle (e.g. Cronin 2004). The detailed elemental composition at the knee and above it is known only very roughly (e.g. Hoerandel 2004; Watson 2001, 2003; Cronin 2004).

The CR arrival directions at energy below \sim EeV are isotropized by the Galactic magnetic fields. At energies well above EeV, their arrival directions may point towards their Galactic sources and at extremely high energies they may point at extragalactic sources. Initial reports of deviations from isotropy in the arrival directions of such cosmic rays with energy above EeV and of some clustering in their arrival directions are still debated (e.g. Watson 2001,2003; Cronin 2004).

The Galactic cosmic ray luminosity exceeds 10^{42} erg s⁻¹ (Dar & De Rújula 2001b).

It is widely believed that Galactic CRs with energy below the knee are accelerated mainly in Galactic supernova remnants (SNRs). The opinions on

the origin of CRs with energy between the knee and the ankle are still divided between Galactic and extragalactic origin. CRs with energy above the ankle are generally believed to be extragalactic in origin because they can no longer be isotropized by the Galactic magnetic fields while their arrival directions are isotropic to a fair approximation. Yet Galactic origin is not ruled out – they may be produced by the decay of unknown massive particles or other unknown sources which are distributed isotropically in an extended Galactic halo. An observational proof that the CRs above the ankle are extragalactic in origin, such as arrival directions which are correlated with identified extragalactic sources or a Greisen-Zatsepin-Kuzmin (GZK) cutoff (Greisen 1966; Zatsepin & Kuzmin 1966) due to π production in their collisions with the cosmic microwave background radiation (MBR), are still lacking (Cronin 2004). Moreover, there is no single solid observational evidence which supports the SNR origin of CRs below the knee (see, e.g. Plaga 2002 and references therein). In fact, the evidence from γ -ray astronomy, X-ray astronomy and radio astronomy strongly suggests that **SNRs are not the major accelerators of CRs with energy below the knee:**

- **SNR origin cannot explain the Galactic CR luminosity:** Radio emission and X-ray emission from SNRs provide strong evidence for acceleration of high energy electrons in SNRs. Some SNRs were also detected in TeV γ -rays which could be produced by the prompt decay of π^0 's from collisions of high energy hadronic cosmic rays with the ambient protons and nuclei in and around the SNR. However, recent observations of SNRs inside molecular clouds (and careful analysis of TeV emission in others) show that the time-integrated CR luminosity of these SNRs does not exceed 10^{48} erg . The rate of SN explosions in the Galaxy which is estimated to be $\sim 1/50 \text{ year}$, yields a total CR luminosity which falls short of the estimated luminosity of the Milky Way (MW) in CRs, $L_{CR}[MW] > 10^{41} \text{ erg s}^{-1}$, by two orders of magnitude.
- **SNR origin cannot explain the diffuse Galactic GBR:** As the CRs from SNRs diffuse through the Galactic magnetic fields, the interactions of CR electrons with ambient photons and of CR nuclei with ambient nuclei in the interstellar medium produce a diffuse background of γ -rays. Such a diffuse gamma background radiation (GBR) has been detected by EGRET and Comptel on board the Compton Gamma Ray Observatory (CGRO). However, the scale length of the distribution of SNR in the Galactic disk is $\sim 4 \text{ kpc}$ and cannot explain the scale length of the observed GBR, which is larger by more

than an order of magnitude (Strong & Mattox 1996). In particular, energetic electrons cool rapidly by inverse Compton scattering of stellar light and of microwave background radiation (MBR). Over their cooling time they cannot reach far enough from the SNRs by diffusion to explain the intensity of GBR at large distances from the Galactic center

- **SNR origin cannot explain the diffuse radio emission from galaxies and clusters:** Because of their fast cooling in the MBR the electrons from SNRs, which are mainly located in the galactic disks, cannot reach large distances from the galactic disks, by either diffusion or non-relativistic winds. The radio emission from our Galaxy, from edge-on galaxies and from the intergalactic space in clusters of galaxies provide evidence for high energy electrons at very large distances from the galactic disks where most of the SNRs are located.

Although supernova remnants (SNRs) do not seem to be the main source of CRs in our Galaxy, in external galaxies and in the intergalactic medium (IGM), SN explosions may still be the main source of CRs at all energies, if SNe emit highly relativistic bipolar jets which produce the visible GRBs when they point in our directions (Dar 1998a; Dar and Plaga 1999)¹. Here, I will outline briefly a simple theory of the origin of CRs at all energies, which is based on the extremely successful cannonball (CB) model of GRBs (Dar & De Rújula 2000, 2003). Many ideas are adopted from Dar & Plaga 1999. I will show that the theory explains remarkably well the main observed properties of Galactic and extragalactic cosmic rays. A more complete theory and more rigorous derivation of CR properties from the CB model will be published elsewhere (De Rújula and Dar & De Rújula, in preparation). According to this theory:

- CRs with energy below the CR ankle are Galactic in origin. They are ISM particles which were swept up and accelerated by the CBs to a maximal lab energy – the elemental knee – mainly by elastic magnetic

¹The association between GRBs and high energy CRs was first suggested by Dar et al. (1992). Waxman (1995), Vietri (1995) and Milgrom (1995) suggested that extragalactic GRBs accelerate the ultra-high energy cosmic rays (UHECR) observed near Earth while Dar (1998a) and Dar & Plaga (1999), following the first observational evidence for a GRB-SN association (Galama et al 1998), suggested that the bulk of the cosmic rays **at all energies** are accelerated in bipolar jets which are ejected in SN explosions and produce Galactic GRBs, most of which are beamed away from Earth.

deflection in the CBs rest frame. The first knee in the all-particle spectrum is the maximal lab energy of CR protons; the ‘second’ knee is that of the iron group nuclei and heavier metals ².

- A fraction of the CR nuclei which are injected into the ISM with energy below the knee are reaccelerated by CBs from other SN explosions all the way to the highest observed cosmic ray energies. CR nuclei with energy above the ankle are extragalactic in origin. They are galactic CRs which were reaccelerated in the interstellar medium (ISM) by CBs from SN explosions and escaped directly into the intergalactic medium (IGM). They have accumulated there during the Hubble time and were isotropized by the IGM magnetic fields. The ankle is the energy around which magnetic trapping and isotropization of Galactic CRs cease to be efficient, the CRs begin to escape freely into the IGM and the diffuse extragalactic CR flux takes over.
- The galactic CRs which escape into the IGM have a spectral index $p \approx 2.2$ below the knees, and $p \approx 2.7$ above it. At ultra-high energies (UHE), the spectrum of the extragalactic CRs is modified by their interaction with the microwave background radiation (mainly, π production, pair production and photo-dissociation of nuclei) and by the Hubble expansion during their residence time in the IGM.
- The energy deposited in the IGM by the CBs and by their associated CR jets stirs it up and generates the IGM magnetic field.
- The CR electrons, which are accelerated/deposited directly in the IGM, produce an extragalactic diffuse gamma-ray background radiation (GBR) via inverse Compton scattering of the cosmic microwave background (MBR).

2 Collimated jets and relativistic beaming

Radio, optical and X-ray observations with high spatial resolution indicate that relativistic jets, which are fired by quasar and microquasars, are made of a sequence of plasmoids (cannonballs) of ordinary matter whose initial expansion (presumably with an expansion velocity similar to the speed of

²Jets from microquasars and active galactic nuclei may also contribute significantly to CR acceleration in galaxies, and in clusters of galaxies (e.g. Dar 1998b; Heinz & Sunyaev 2002), but they will not be discussed here.

sound in a relativistic gas) stops shortly after launch (e.g., Dar & De Rújula 2003 and references therein). The turbulent magnetic fields in such plasmoids gather and scatter the ionized ISM particles on their path. For the sake of simplicity, we shall assume³ that a fraction of the incident ISM particles are scattered isotropically by the CB and maintain their energy in the CB’s rest frame. Electrons which are trapped in the CB cool there quickly by synchrotron emission. This radiation which is emitted isotropically in the CB’s rest frame is beamed by the relativistic bulk motion of the CBs (Lorentz factor $\gamma = 1/\sqrt{1 - \beta^2}$). Let primed quantities denote their values in the plasmoid’s rest frame and unprimed quantities their corresponding values in the lab frame. Then the angle θ' of the emitted photons in the CB’s rest frame relative to the CB’s direction of motion, and the corresponding angle θ in the lab frame, are related through:

$$\cos \theta' = \frac{\cos \theta - \beta}{1 - \beta \cos \theta}. \quad (1)$$

This relation is valid to a good approximation also for the emission of highly relativistic massive particles. When applied to an isotropic distribution of emitted particles in the CB’s rest frame, it yields a distribution,

$$\frac{dn}{d\Omega} = \frac{dn}{d\Omega'} \frac{d\cos\theta'}{d\cos\theta} \approx \frac{n}{4\pi} \delta^2 \quad (2)$$

in the lab frame where

$$\delta = \frac{1}{\gamma(1 - \beta \cos \theta)} \quad (3)$$

is the Doppler factor of the CB motion viewed from a lab angle θ . For plasmoids with highly relativistic bulk motion Lorentz factor, $\gamma^2 \gg 1$, and for $\theta^2 \ll 1$, the Doppler factor is well approximated by

$$\delta \approx \frac{2\gamma}{1 + \gamma^2 \theta^2}. \quad (4)$$

Hence, the isotropic distribution of the emitted particles in the CB’s rest frame is collimated into a narrow conical beam, “the beaming cone”, around the direction of motion of the CB in the lab frame,

$$\frac{dn}{d\Omega} \approx \frac{n}{4\pi} \left[\frac{2\gamma}{1 + \gamma^2 \theta^2} \right]^2. \quad (5)$$

³Acceleration in the CB’s rest frame and deviation from isotropic scattering have been studied by A. De Rújula, 2004, in preparation

The beaming depends only on the CB's Lorentz factor and not on the mass of the scattered particles.

Ambient ISM particles which are practically at rest in the ISM, enter the CBs with an energy $E' = \gamma m$. After magnetic scattering and isotropization in the CB they are emitted with a lab energy

$$E = \gamma E' (1 + \beta^2 \cos\theta'). \quad (6)$$

Their energy distribution in the lab frame is given by a simple step function:

$$\frac{dn}{dE} = \frac{dn}{d\cos\theta'} \frac{d\cos\theta'}{dE} \approx \frac{n}{2\beta^2\gamma^2 m} \Theta(E - 2\gamma^2 m), \quad (7)$$

where $\Theta(x) = 1$ for $x < 1$ and $\Theta(x) = 0$ for $x > 1$. The accelerated nuclei ($m = A m_p$) and electrons ($m = m_e$), which are initially ejected into a narrow cone, are later scattered and isotropized by the galactic magnetic fields. They do not reach far away from their injection cone before they radiate most of their initial energy via synchrotron emission and inverse Compton scattering of the microwave background photons along their direction of motion. Their radiation, which is beamed along their motion, can be seen by an observer outside the CBs' beaming cone, only when their direction of motion points towards him. Because of the fast radiative cooling of energetic electrons, their radiation is visible mainly when they are still within/near the beaming cone. The gradual increase of the opening angle of the injection cone due to jet deceleration, together with the finite lifetime of the radiating electrons which confines them to near the jet, produce the conical images of radio and optical jets. It is often confused with the true geometry of the relativistic jet, which reveals itself only in observations at much higher frequencies where the observed emission requires much stronger magnetic fields than those present in the ISM and IGM.

3 CR acceleration by decelerating jets

Let n_A be the density of nuclei of atomic mass A along the jet trajectory. Let us assume that the elemental abundances $X_A = n_A/n_b$ are constant along the jet trajectory, where n_b is the total baryon density. Let us define a total effective mass of these particles, $\bar{m} = m_p \sum A X_A$. Let us assume that most of them are swept into the jet. Let us also neglect the small energy radiated away by the swept up electrons except for the fact that it ionizes completely the ISM in front of the jet. Then, energy conservation implies that $M(x) \gamma(x) = M_0 \gamma_0$ where $M(x)$ and $\gamma(x)$ are the total rest-mass

and bulk-motion Lorentz factor of the jet along its trajectory with initial values, $M_0 = M(0)$ and $\gamma_0 = \gamma(0)$, respectively. Let us denote by $dN_A(x)$ the number of cosmic ray nuclei of atomic mass A which are accelerated promptly by isotropic scattering in the CB rest frame at distance x . Noting that their average lab energy is $\gamma^2 A m_p$, one can write the approximate deceleration law due to CR acceleration as:

$$M d\gamma = -dN_b \bar{m} \gamma^2, \quad (8)$$

or

$$dN_A \approx \frac{X_A M_0 \gamma_0}{\bar{m}} \frac{d\gamma}{\gamma^3}. \quad (9)$$

Note that Eq. (8) depends neither on the geometry of the jet nor on the density profile along the jet trajectory. The CR energy spectrum generated by a decelerating jet can be obtained by replacing n_p in Eq. (7) by dn_A and integrating over γ at a fixed E under condition (6):

$$\frac{dN_A}{dE} = \frac{X_A M_0 \gamma_0}{2 A m_p \bar{m}} \int \frac{d\gamma}{\gamma^5} \propto \frac{X_A}{A \bar{m}} \left[\left[\frac{E}{A m_p} \right]^{-2} - \left[\frac{E_{max}}{A m_p} \right]^{-2} \right] \Theta(E - E_{max}), \quad (10)$$

where,

$$E_{max} = 2 A m_p \gamma_0^2 \quad (11)$$

is the maximum energy gained by nuclei at rest in the ISM, in a **single scattering**. Thus, for energies well below E_{max} , the injected spectrum of CRs is a simple power-law, $dN_A/dE \sim E^{-2}$. The effective power on the rhs of Eq. (8) may be increased slightly by the scattering of ISM particles by the ambient magnetic field which is swept up by the CRs that were scattered by the CB (to a mean Lorentz factor γ^2). Then the mean Lorentz factor of these secondary accelerated particles is γ^4 . Such a multiple acceleration has been assumed to take place within relativistic shocks in collisionless shock acceleration. A modified acceleration law,

$$M d\gamma = -dN_b \bar{m} \gamma^{2.4}, \quad (12)$$

is needed in order to generate a slightly steeper power-law spectrum, $dN_A/dE \sim E^{-2.2}$, which was deduced from the spectrum of the diffuse gamma ray emission by Galactic cosmic ray electrons (e.g. Dar and De Rújula 2001a) and from the diffuse radio emission from cosmic ray electrons in our galaxy, in external galaxies and in clusters of galaxies. It has been claimed that such a power-law index arises in numerical calculations

of CR acceleration in collisionless shock acceleration (Bednarz & Ostrowski 1998; Kirk et al. 2000). In the following, we shall assume that the injection spectrum of CRs by relativistic jets has a spectral index $p \approx -2.2$.

4 Spectral steepening by magnetic trapping

The cosmic rays which are accelerated by the highly relativistic jets from SN explosions are initially beamed into narrow cones along the jets' trajectories. Their free escape into the intergalactic space is delayed by diffusion in the galactic magnetic fields which isotropize their direction of motion. The accumulation of CRs during their trapping/residence time in the galaxy, which decreases with increasing energy, steepens their energy spectrum. During their galactic residence, CRs also lose energy via Coulomb and inelastic collisions and gain energy through Fermi acceleration by galactic winds and jets. We shall first neglect reacceleration of CRs in the ISM and their inelastic interactions there, and correct only for accumulation during residence time. The Larmor radius of CRs with an electric charge Z in a magnetic field B is given by

$$R_L = \frac{\beta E}{e Z B} \approx \left[\frac{E}{PeV} \right] \left[\frac{1}{Z B_{\mu G}} \right] pc, \quad (13)$$

where $B_{\mu G}$ is the magnetic field strength in $\mu Gauss$. The energy-dependent diffusion of CRs due to pitch-angle scattering with a Kolmogorov and Kraichnan spectrum of MHD turbulence results in a CR residence time in the host galaxy which behaves (e.g. Wick, Dermer & Atoyan 2003) like $(E/Z)^{-0.5}$. Thus, the accumulation of CRs before their escape steepens the injection spectral index, $p = -2.2$, by 0.5 to $p = -2.7$, yielding,

$$\frac{dN_A}{dE} \propto \frac{X_A(E/A) A^{1.2} Z^{0.5}}{\bar{m}} \left[\frac{E}{m_p} \right]^{-0.5} \left[\left[\frac{E}{m_p} \right]^{-2.2} - \left[\frac{E_{max}}{m_p} \right]^{-2.2} \right] \Theta(E - E_{max}). \quad (14)$$

The decreasing metallicity and the deceleration of the jet along the jet's trajectory result in an effective energy dependent $X_A(E/A)$ which is discussed in section 7. Eq. (14) ignores acceleration inside the CBs and reacceleration of CRs in the ISM by the CBs. Such effects will be included phenomenologically in section 9.

5 CRs from SN jets

There is mounting observational evidence that long duration gamma ray bursts (GRBs) are produced by ultra-relativistic jets of ordinary matter which are ejected in core collapse supernova (SN) explosions (see e.g. Dar 2004; Dado these proceedings) as long advocated by the remarkably successful CB model of GRBs (e.g., Dar & De Rújula 2000, 2003; Dado et al. 2002, 2004 and references therein). In the CB model, the long-duration GRBs are produced in ordinary core-collapse SN explosions. Following the collapse of the stellar core into a neutron star or a black hole, and given the characteristically large specific angular momentum of stars, it is hypothesized that an accretion disk or torus is produced around the newly formed compact object, either by stellar material originally close to the surface of the imploding core and left behind by the explosion-generating outgoing shock, or by more distant stellar matter falling back after its passage (De Rújula 1987). A CB is emitted, as observed in microquasars, when part of the accretion disk falls abruptly onto the compact object (e.g. Mirabel & Rodriguez 1999; Rodriguez & Mirabel 1999 and references therein). The high-energy photons of a single pulse in a GRB are produced as a CB coasts through the “ambient light” permeating the surroundings of the parent SN. The electrons enclosed in the CB Compton up-scatter photons to energies which, close to the CBs direction of motion, correspond to the γ -rays of a GRB and less close to it to the X-rays of an XRF. Each pulse of a GRB corresponds to one CB in the jet. The timing sequence of emission of the successive individual pulses (or CBs) reflects the chaotic accretion process and its properties are not predictable, but those of the single pulses are (Dar & De Rújula 2003 and references therein). The initial Lorentz factors of the CBs were deduced from cannonball model analysis of GRBs and their afterglows (Dar & De Rújula 2003). Their distribution, and the corresponding distribution of E_{max} , can be well approximated by a log-normal distribution:

$$P(E_{max}) \approx \frac{1}{E_{max} \sigma \sqrt{2\pi}} \exp \left[-\frac{(\ln E_{max} - \ln \bar{E}_{max})^2}{2\sigma^2} \right]. \quad (15)$$

The energy-spectra of the individual CR elements is obtained by integrating Eq. (14) over E_{max} with the log-normal distribution (15):

$$\frac{dN_A}{dE} \rightarrow \int P(E_{max}) \frac{dN_A}{dE} dE_{max}. \quad (16)$$

So far we have ignored acceleration inside the CBs and reacceleration of CRs in the ISM by the CBs. Such effects will be included in the following sections.

6 The CR knees

The log-normal distribution of the Lorentz factors of CBs, as inferred from GRBs (Dar & De Rújula 2003), produce a relatively narrow distribution of the maximum energy of CRs produced by elastic magnetic scattering of ambient ISM particles in the CB. Thus, the energy spectra of the individual CR nuclei, integrated over all CBs, retain a sharp knee at

$$E_{knee} \approx \bar{E}_{max} = 2 A m_p \bar{\gamma}_0^2 \approx 3 A PeV. \quad (17)$$

This is shown in Fig. (3) which compares the predicted energy spectra of H, He, and Fe group nuclei around their respective knees as calculated⁴ from Eqs. (14), (16), (17), and those extracted from the Cascade observations (Kampert et al. 2004; Hoerandel et al. 2004). Despite the large experimental uncertainties, the theory seems to reproduce correctly the elemental knees, their A-dependence and their energy spectrum around these knees. Note that the predicted knee for different elements is proportional to A rather than to Z as in conventional models based on shock acceleration, where the maximum energy gain is limited by the requirement that the size of the accelerator be larger than the Larmor radius of the accelerated CR particles. This difference is large only for protons, deuterium and very heavy nuclei. It appears to be supported by the data, but more accurate values for the knee energy of different nuclei are needed from the CR experiments in order to draw a reliable conclusion.

7 Elemental abundances and spectral indices below the knees

The enhancement in the abundance of CR nuclei as function of nuclear mass, charge and CR energy below the elemental knee, which is predicted by the CB model, can be read from Eq. (14),

$$X_A[CR] \sim X_A(E/A) A^{1.2} Z^{0.5}, \quad (18)$$

where $X_A(E/A)$ is roughly the element's abundance encountered on the average by the CBs along their trajectory in the ISM around a distance where the CB Lorentz factor is $\gamma \approx E/A m_p$. The A-dependence follows from the fact that all CR nuclei, which are accelerated by CBs, have the

⁴For the sake of simplicity, Fermi acceleration inside the CBs was roughly approximated by an effective σ which was fixed by a best fit to the proton data.

same universal Lorentz factor distribution. The Z -dependence follows from the dependence of Galactic magnetic-trapping time of CRs on their Larmor radius.

More than 90% of SN explosions take place in star formation-regions which are enclosed in superbubbles (SB) formed by the ejecta from former SN explosions and massive stars. Therefore, near the GRB site, the elemental abundances X_A are typically that of young SNRs (which are made of SN ejecta + progenitor ejecta prior to the SN). Further down they become typical SB abundances. Both $X_A[SNR]$ and $X_A[SB]$ are poorly known. Outside the SB, they become normal ISM abundances and when the jet enters the halo, X_A become typical halo abundances. The decrease in metallicity along the CB trajectories, approximately by a factor of a few, induces a noticeable change in the spectral index of the different CR elements. It makes the proton spectrum slightly steeper and decreases slightly the steepness of the energy spectrum of the metals. The change in the spectral index, is given roughly by

$$p_A \approx 2.7 + \frac{\Delta[\log X_A[E/A]]}{\Delta[\log(E/A)]}. \quad (19)$$

The change Δ in elemental abundances along the CB trajectory from $X_A[ISM] \approx X_A[\odot]$ (given e.g. by Grevesse & Sauval 1998) to $X_A \sim X_A[SNR]$ corresponds to an energy-increase from $E \sim m_A$ to $E \sim E_{max}[A]$. Thus, for protons, $p_1 \approx 2.75$ below the proton knee, while for iron nuclei below the iron knee, $p_{56} \approx 2.62$. In Fig. 2 we compare the predicted spectral index below the knee for different elements and their observed values as reported by Wiebel-Sooth et al. (1998) from their best fits to the world CR data below the knee. The CB model prediction for all the abundant elements above He is described approximately by the interpolation, $p_A \sim 2.70 - 0.02 \ln A$.

During their residence time in galaxies, spallation of CRs in collisions with ISM nuclei increases significantly the abundances of long-lived rare elements, but changes only slightly the abundances of the most abundant elements. A detailed discussion of the effects of spallation on CR elemental abundances is beyond the scope of this paper. Thus, Table I presents the observed CR elemental abundances near TeV energy and $K_A[SB] = X_A[SB]/X_A[\odot]$ the enhancement in the abundance of the the most abundant elements in SBs relative to their solar abundances, which is needed in the CB model to explain the observed CR abundances. Indeed, these enhancements are consistent with an expected SB metallicity ~ 5 times solar (Lingenfelter et al. 2001) and with those extracted from X-ray spectra

of SBs measured by XMM newton (with large uncertainties). Table I also lists the values of $X_A[ISM] \approx X_A[\odot]$ which we used in the CB model calculations. Note the large enhancement in the abundance of helium and the huge enhancements in the abundances of the metals in CRs compared to their ISM and solar values. Ignoring spallation, the CB model reproduces very well these very large enhancements.

Above the proton knee, CRs become progressively poor in protons. Above the *He* knee, they become poor also in *He*, then also in *CNO*, etc., until near the iron knee (the second knee) where they consist mainly of iron and heavier elements. Spallation affects only slightly the value of $\langle \ln A \rangle$. This is shown in Fig. 4 where the CB model prediction for $\langle \ln A \rangle$ as a function of CR energy is compared with its value as inferred from various observations (see, e.g. Hoerandel). The effects of spallation were neglected in the CB model predictions. Despite the large spread in the world data, the CB model clearly reproduces the observed trends.

The energy spectrum of individual elements falls rapidly at their knees. The all-particle CR spectrum beyond the proton knee loses progressively the contribution from heavier and heavier elements, until it becomes almost pure iron. This produces a steepening of the spectrum between the proton knee and the iron knee and results in a composition which gradually approaches a pure iron+heavier metals composition as shown in Fig. 4. Because the abundances of elements heavier than iron are rather small compared to iron, **the all-particle spectrum steepens again at the iron knee forming the second knee** in the all-particle spectrum. Beyond the second knee, reacceleration of CRs in SBs become the main source of CRs.

8 The maximal energy of reaccelerated CRs

A cosmic ray in the ISM with an energy E_L which collides with a CB at angle θ_L relative to the direction of motion of the CB, has an energy $E' = \gamma E_L (1 - \beta \beta_L \cos \theta_L)$ in the CB rest frame. If it is scattered elastically and emitted at angle θ' in the CB rest frame, its energy in the ISM rest frame becomes

$$E = \gamma^2 E_L (1 + \beta' \beta \cos \theta') (1 - \beta \beta_L \cos \theta_L). \quad (20)$$

However, CBs can accelerate CRs as long as their Larmor radius in the CB rest frame is smaller than the CB's radius, R_{cb} , i.e., E' must satisfy, $E' \leq e Z B R_{cb}$. Hence, the maximal energy of CR nuclei accelerated directly by/in CBs is

$$E_{max} \approx 4 \gamma e Z B R_{cb}. \quad (21)$$

This relation differs from the usual ‘Hillas relation’ by the factor 4γ which is due to the relativistic motion of the CR accelerator – the CB. For a magnetic field whose pressure is equal to that of the scattered ISM particles (Dado et al. 2002), $B \approx \gamma \sqrt{2\pi n_p \bar{m}}$, where n_p is the superbubble density, the maximal energy is,

$$E_{max}[A] \approx 4 \times 10^{20} Z \left[\frac{\gamma_0^2}{10^6} \right] \left[\frac{n_p}{10^{-3} \text{ cm}^{-3}} \right] \left[\frac{R_{cb}}{10^{14} \text{ cm}} \right] eV. \quad (22)$$

Hence, SN jets which produce GRBs can accelerate CR nuclei to energies much higher than the highest energy of a cosmic ray which has ever been measured, $\sim 3.2 \times 10^{20} eV$ (Bird et al. 1995).

9 Reacceleration of CRs by CBs

CRs which are injected into the ISM and IGM by SN jets can be reaccelerated later by magnetic scattering from highly relativistic jets (CBs) from other SN explosions. This reacceleration could have been taking place since the beginning of star formation. Detailed treatment of reacceleration is beyond the scope of this paper. A rough estimate of the energy spectrum of CRs resulting from reacceleration of CRs in SBs by magnetic scattering from CBs can be obtained by following the calculation of the spectrum of CRs produced by CBs through magnetic scattering of ISM particles at rest. One has to replace m in Eq. (6) by $\gamma E_L (1 - \beta \cos\theta_L)$ and integrate over the CR spectrum as given by Eqs. (14), (16) and over $\cos\theta_L$, subject to Eq. (20). An approximate integration yields a population of reaccelerated CRs above the CR knees with an energy spectrum,

$$\frac{dN_A}{dE} \propto \left[\frac{E}{m_p} \right]^{-p_A}, \quad (23)$$

which extends up to $E \approx E_{max}[A]$ given by Eq. (22). Because of the steep decline with energy, $\sim E^{-2.7}$, of the CR spectrum below the CR knee, most of the CRs nuclei with energy $E > E_{knee}$ were reaccelerated in SBs from an initial CR energy $\sim E/\gamma_0$ to their final energy E . Because the energy E of reaccelerated CRs, depends only on the energy in the CB rest frame, and not on their mass or charge (as long as $E < E_{max}[A]$), the composition of reaccelerated CRs is approximately the CR composition at the all-particle CR knee.

10 The CR ankle and beyond

In a steady state, the bulk of the extragalactic CRs are injected into the IGM with their galactic injection spectrum i.e., a power-law spectrum with a spectral index $p = p_A - 0.5$ below the elemental knee and $p = p_A$ above it, all the way to E_{max} . During the Hubble time, this spectrum is modified by the cosmic expansion and by pair production, photoproduction and photodissociation on the MBR photons (see e.g., Stecker & Salamon 1999). In the CB model the CR ankle is the energy where the residence time of cosmic rays in the Galaxy approaches the free escape time. This happens when the Larmor radius of the CRs approaches the coherence length of the turbulent Galactic magnetic fields (Dar & Plaga 1999). Hence, the elemental ankles satisfy $E_{ank}[A] = Z E_{ank}[p]$. The exact value of $E_{ank}[p]$ cannot be calculated from first principles and is treated as an adjustable parameter. Beyond the ankle, the CR energy spectrum is dominated by the flux of the CRs from the IGM which have been injected there by SN explosions in galaxies in the local super cluster since the beginning of star formation, and were isotropized by the IGM magnetic fields. The contribution of CR-reacceleration to the observed elemental CR flux, well above the knee, can be written as,

$$\frac{dN_A}{dE} \propto \frac{X_A[SB] A^{1.2} Z^{0.5}}{\bar{m}} \left[\frac{E}{m_p} \right]^{-p_A} \left(\left[\frac{E}{E_{ank}[A]} \right]^{-0.5} + 1 \right) \exp(-E/E_0[A]), \quad (24)$$

where $E_0[A] \approx E_{GZK}[A] \sim 5 \times 10^{19} A eV$ is the effective CR cutoff due to photo-production of π (the GZK cutoff) or photo-dissociation of nuclei (Puget, Stecker & Bredekamp, 1976; Stecker & Salamon 1999) on the MBR photons. Below $E_{max}[A]$, reacceleration is blind to A and Z . Consequently, the proportionality constant in Eq. (24) is independent of A and Z . At the ankle the CRs residence time in the Galaxy is approximately their free escape time from the Galaxy. This is described by the factor $[(E/E_{ank})^{-0.5} + 1]$ on the rhs of Eq. (24). The accumulation time of CRs in the IGM is roughly the age of the Universe, $t_H \sim 14 Gy$. The average IGM volume in the local Universe per Milky Way-like galaxy is $\bar{V} \sim 100 Mpc^3$, while the volume of the Galactic CR halo is roughly (Dar & De Rújula 2001b) $\bar{V} \sim 10^5 kpc^3$. Thus, ignoring redshift and stellar evolution (which tend to compensate each other), the extragalactic (EG) flux near the CR ankle must satisfy roughly,

$$\frac{dN_{EG}}{dE} \sim \frac{t_H}{t_{esc}} \frac{V_G}{\bar{V}} \frac{dN_G}{dE} \sim \frac{dN_G}{dE}. \quad (25)$$

This relation is nominally satisfied if the mean escape time of CRs from the Galaxy at the ankle is, $t_{esc} \approx 13,500 y$. The spectral index of UHECRs above the ankle can be predicted also from a general consideration: Below the ankle, magnetic trapping increases the CR index by 0.5. The measured spectral index below the ankle is $p \approx 3.2$. Thus, free escape of CRs changes it to $p \approx 3.2 - 0.5 = 2.7$ at the ankle.

In conclusion, in the simple version of the CB model, reacceleration leads to four major predictions:

- The elemental spectral index of UHECRs above the ankle is identical to that below the knee, p_A and consequently the all-particle spectral index above the all-particle ankle is approximately 2.7 .
- The elemental composition of UHECRs above the ankle and below the effective energy thresholds for photoproduction/photodissociation in collisions with the MBR photons is similar to that of CRs below the CR knee.
- The CR spectrum steepens at the GZK cutoff.
- The CR spectrum above the ankle remains highly isotropic up to the GZK cutoff.

The all-particle CR spectrum between 10^2 GeV and 10^{12} GeV as predicted by the CB model is compared in Fig. 1 with the world data as compiled by Ulrich (Kampert et al. 2004). Despite the large uncertainties in the experimental data, and in the model input parameters (e.g. SB abundances, photo-nuclear cross sections), the agreement between theory and experiments appears to be quite good. Note in particular that the predictions above 10^{11} GeV are sensitive to the assumed photo-nuclear cross sections, cosmological model and past SN rates in the local supercluster.

11 The Galactic CR Luminosity

In a steady state, the escape rate of Galactic CRs into the IGM is equal to their production rate. In the CB model, most of the kinetic energy of SN jets is converted to CR energy in the Galaxy. In the CB model, this energy was estimated Dar & De Rújula 2000, 2003) to be $E_k \sim 2 \times 10^{51} erg$ per SN. Thus, a galactic SN rate of $R_{SN} \sim 1/50 y^{-1}$ generates a Galactic CR luminosity of

$$L_{cr}[MW] = R_{SN} E_k \sim 1.1 \times 10^{42} erg s^{-1}. \quad (26)$$

Traditional estimates, which are based on an assumed $\sim 10\%$ conversion of the kinetic energy of the non-relativistic ejecta in SN explosions to CR energy through collisionless shock acceleration, give $L_{cr} < 10^{41} \text{ erg s}^{-1}$.

12 IGM magnetic field

In the CB model, practically all the kinetic energy of the SN jets (CBs), $E_k \sim 2 \times 10^{51} \text{ ergs}$ per SN explosion ends up in the IGM (Dar & Plaga 1999; Dar & De Rújula 2000,2003). The energy and momentum deposited in the IGM may stir it up and generate the IGM magnetic fields. If their energy is equipartitioned with the IGM plasma (primordial matter and galactic winds) and the IGM magnetic fields then, neglecting cosmic-evolution corrections, the energy density of these fields is roughly given by,

$$B \sim \left[\frac{8\pi R_{SN} E_k}{3 H_0} \right]^{1/2} \approx 20 \text{ nGauss}, \quad (27)$$

where $R_{SN} \approx 6 \times 10^{-5} \text{ Mpc}^{-3} \text{ y}^{-1}$ is the total rate of SN explosions per unit volume in the local universe and $1/H_0 \approx 14 \text{ Gy}$ is the approximate age of the Universe. If only SNIb/Ic produce relativistic jets/GRBs then $B \sim 10 \text{ nGauss}$. These rough estimates are consistent with estimates based on measurements of Faraday rotation of polarized light from distant quasars.

13 The extragalactic GBR produced by CRe

Inverse Compton scattering of CR electrons (CRe) in external galaxies and in the IGM produces an isotropic GBR with a canonical spectrum $dn_\gamma/dE \sim E^{-2.1}$ whose magnitude has been estimated in Dar & De Rújula 2001a to be less than 40% of the diffuse gamma ray background radiation at high Galactic latitudes. This component should be detected by GLAST. Such an extragalactic component will reduce the CR luminosity of the Milky Way Galaxy, $L_{cr}[MW] = 6.8 \times 10^{42} \text{ erg s}^{-1}$, as estimated by Dar & De Rújula (2001), by a factor of $[0.6]^3$ to the value $L_{cr}[MW] = 1.5 \times 10^{42} \text{ erg s}^{-1}$, similar to that estimated in Eq. (26).

14 conclusions

The CB model of GRBs was used to show that the bipolar jets from SN explosions are the main origin of cosmic rays at all energies. The CB model

correctly predicts, within the experimental uncertainties, the observed all-particle CR flux, its energy spectrum and its elemental composition as function of energy. At ultra-high energies above the CR ankle, for which the Galactic magnetic fields can no longer delay the free escape of CRs from the Galaxy, the UHECRs which were injected there over the Hubble time by SN jets from all the galaxies in the local supercluster and were isotropized there by the IGM magnetic fields, dominate the Galactic CR spectrum. A GZK cutoff due to the interaction of UHECRs with the microwave background radiation is expected. The CR nuclei which diffuse out of galaxies, or are directly deposited in the IGM by the relativistic SN jets, may be the origin of the IGM magnetic fields. Inverse Compton scattering of MBR photons by the CR electrons in the IGM produce a diffuse extragalactic gamma-ray background radiation. It seems that the 92 years old puzzle of the origin of Galactic CRs may have been solved, but more precise CR data on the energy spectrum of individual nuclei, from the elemental knees all the way well above the GZK cutoff, and astrophysical data on the elemental composition of SNRs and SBs, as well as more precise CB model calculations which include CR interactions with the ambient matter and radiation in the ISM and the IGM are needed to secure this conclusion.

Acknowledgements: The author would like to thank Shlomo Dado and Alvaro De Rújula for a long term collaboration in the development of the CB model for GRBs and CRs, Jacques Goldberg for technical help and the organizers of La Thuile 2004 meeting and the Vulcano 2004 Workshop for their warm hospitality, excellent organization and very interesting scientific programs. The support of the Asher Space Research Institute at the Technion is gratefully acknowledged. This research was not supported by the Israel Science Foundation for basic research.

References

- [1] Bednarz, J. & Ostrowski, M. 1998, PRL, 80, 3991
- [2] Biermann, P., & Sigl. G., 2001, Lect. Notes Phys. 576, 1
- [3] Bird, D. J., et al. 1995, ApJ, 441, 144
- [4] Cronin, W. J. 2004, astro-ph/0402487
- [5] Dado, S., Dar, A. & De Rújula, A. 2002, A&A, 388, 1079
- [6] Dar, A. 1998b, astro-ph/9809163
- [7] Dar, A. 1998a, Proc. XIIth Workshop on Perspectives in Particle Physics' (ed. M. Greco) Aosta Valley, p. 23, March 1-7, 1998, Italy
- [8] Dar, A. & De Rújula, A. 2000, astro-ph/0008474
- [9] Dar, A. & De Rújula, A. 2001a, MNRAS 323, 391

- [10] Dar, A. & De Rújula, A. 2001b, ApJ, 547, L33
- [11] Dar, A. & De Rújula, A. 2003, astro-ph/0308248
- [12] Dar, A. & Plaga, R. 1999, A&A, 349, 259
- [13] Dermer, C. D. & Humi, M. ApJ. 2001, 556, 479
- [14] De Rújula, A. 1987, Phys. Lett., 193, 514
- [15] Greisen, K., 1966, PRL, 16, 748
- [16] Grevesse, N. & Sauval, A. J. 1998, Space Sci. Rev. 85, 161
- [17] Heinz, S. & Sunyaev, R. A. 2002, A&A, 390, 751
- [18] Hoerandel, J. R., 2004, astro-ph/0402356 and these proceedings
- [19] Kampert, K. H. et al. 2004, astro-ph/0405608
- [20] Kirk, J. G., Guthmann, A. W., Gallant, Y. A., Achtenberg, A. 2000, ApJ. 542, 235
- [21] Lingenfelter, R. E., Higdon, J. C. & Ramaty, R. 2000, AIPC, 528, 375
- [22] Nagano, A., Watson, A. A., 2000, RMP, 72, 689
- [23] Milgrom, M. & Usov, V. 1996, Astropart. Phys. 4, 365.
- [24] Mirabel, I. F. & Rodríguez, L. F. 1999, ARA&A, 37, 409
- [25] Olinto, A. V. 2004, astro-ph/0404114
- [26] Plaga, R. 2002, NA, 7, 317
- [27] Puget, J. L., Stecker, F. W. & Bredekamp, J. H. 1976, ApJ, 205, 638
- [28] Rodríguez, L. F. & Mirabel, I. F. 1999, ApJ, 511, 398
- [29] Stecker, F. W. & Salamon, M. H. 1999, ApJ, 512, 521
- [30] Strong, A. W. & Mattox J. R. 1996, A&A 308, L21
- [31] Vietri, M. 1995, ApJ. 453, 883
- [32] Waxman, E. 1995, PRL 75, 386
- [33] Wiebel-Sooth, B., Biermann, P. L. & Meyer, H. 1998, A&A, 330, 389
- [34] Watson, A. A. 2001, AIPC, 586, 817
- [35] Watson, A. A. 2003, in Astronomy, Cosmology and Fundamental Physics, Proceedings of the ESO-CERN-ESA Symposium held in Garching, Germany, 4-7 March 2002, p. 216.
- [36] Zatsepin, G. T., Kuzmin, V. A. 1966, JETP Lett. 4, 78

Table 1: Elemental abundances in the ISM and in CRs at 1 TeV and their predicted enhancement, $K_A[SB]$, in supernova remnants and galactic superbubbles.

Element	$X_A[\odot]$	$X_A[CR]$	$K_A[SB]$
H	0.915 ± 0.005	0.433 ± 0.015	0.47
He	0.083 ± 0.005	0.270 ± 0.007	0.43
Li	$1.15 \pm 0.11 10^{-11}$	$7.82 \pm 0.19 10^{-3}$	
Be	$2.26 \pm 0.23 10^{-11}$	$1.78 \pm 0.18 10^{-3}$	
B	$4.58 \pm 0.46 10^{-10}$	$3.36 \pm 0.30 10^{-3}$	
C	$3.01 \pm 0.68 10^{-4}$	$3.98 \pm 0.04 10^{-2}$	2.73
N	$7.61 \pm 0.15 10^{-5}$	$8.83 \pm 0.30 10^{-3}$	1.85
O	$6.18 \pm 1.09 10^{-4}$	$5.15 \pm 0.15 10^{-2}$	1.05
F	$2.89 \pm 0.29 10^{-8}$	$1.23 \pm 0.18 10^{-3}$	
Ne	$1.098 \pm 0.18 10^{-4}$	$1.73 \pm 0.37 10^{-2}$	1.35
Na	$1.96 \pm 0.16 10^{-6}$	$2.83 \pm 0.12 10^{-3}$	
Mg	$3.48 \pm 0.50 10^{-5}$	$3.01 \pm 0.98 10^{-2}$	5.5
Al	$2.70 \pm 0.57 10^{-6}$	$4.25 \pm 0.57 10^{-3}$	
Si	$3.25 \pm 0.61 10^{-5}$	$2.99 \pm 0.56 10^{-2}$	4.5
P	$2.58 \pm 0.83 10^{-7}$	$1.02 \pm 0.75 10^{-3}$	
S	$1.33 \pm 0.26 10^{-5}$	$8.64 \pm 0.90 10^{-3}$	2.53
Cl	$1.96 \pm 0.24 10^{-7}$	$1.10 \pm 0.07 10^{-3}$	
Ar	$1.92 \pm 0.10 10^{-6}$	$3.14 \pm 0.02 10^{-3}$	4.60
K	$1.21 \pm 0.36 10^{-7}$	$2.02 \pm 0.06 10^{-3}$	
Ca	$2.09 \pm 0.12 10^{-6}$	$5.44 \pm 0.45 10^{-3}$	6.96
Sc	$1.35 \pm 0.14 10^{-9}$	$1.14 \pm 0.07 10^{-3}$	
Ti	$9.6 \pm 0.36 10^{-8}$	$4.25 \pm 0.53 10^{-3}$	
V	$9.15 \pm 0.92 10^{-9}$	$2.36 \pm 0.11 10^{-3}$	
Cr	$4.28 \pm 0.36 10^{-7}$	$5.11 \pm 0.45 10^{-3}$	
Mn	$2.25 \pm 0.20 10^{-7}$	$5.07 \pm 0.53 10^{-3}$	
Fe	$2.89 \pm 0.38 10^{-5}$	$6.69 \pm 0.67 10^{-2}$	3.62
Co	$7.61 \pm 0.16 10^{-8}$	$2.82 \pm 0.26 10^{-4}$	
Ni	$1.62 \pm 0.19 10^{-6}$	$3.74 \pm 0.16 10^{-3}$	3.33

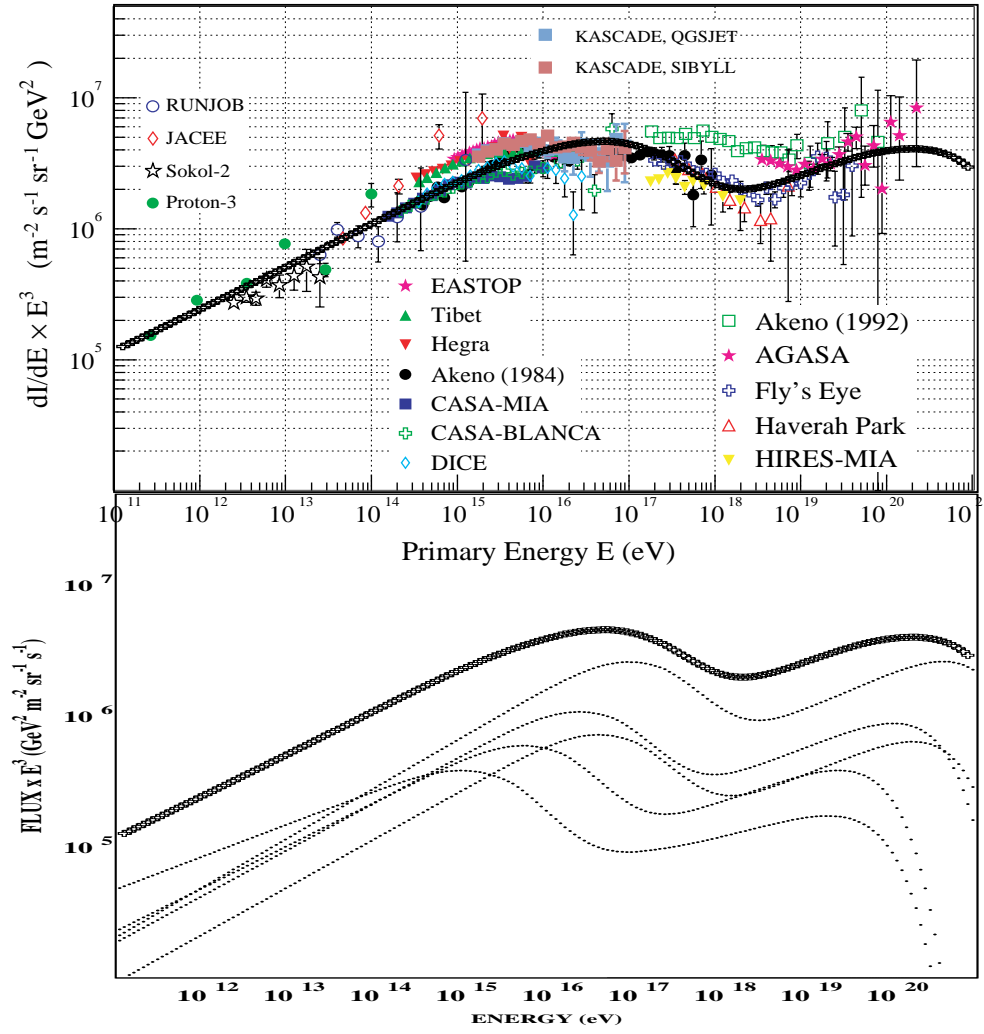


Figure 1: Top: Comparison between the CB model prediction for the all-particle CR spectrum (crosses) and the world data as compiled by Ulrich (Kampert et al. 2004). Bottom: The break down of the CB model prediction for the all-particle CR spectrum (crosses) into the contributions from the most abundant nuclei (lhs, top to bottom): H, He, CNO, Ne-Ca and Fe group nuclei. The theoretical predictions and the observations have been multiplied in both figures by E^3 to emphasize significant deviations from a single power-law decline over thirty orders of magnitude.

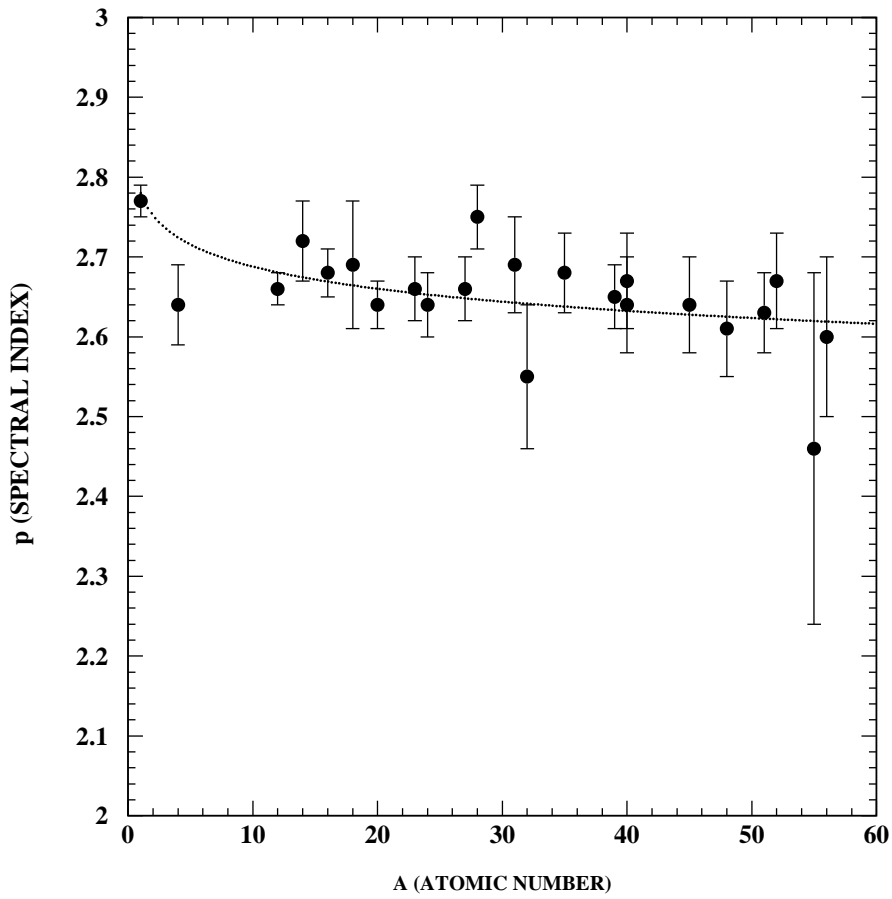


Figure 2: Comparison between the CB model prediction for the A-dependence of the spectral index of CRs for energies below the elemental CR knees, Eq. (18), and their values obtained by Wiebel-Sooth et al. (1997) from best fits to the world CR data.

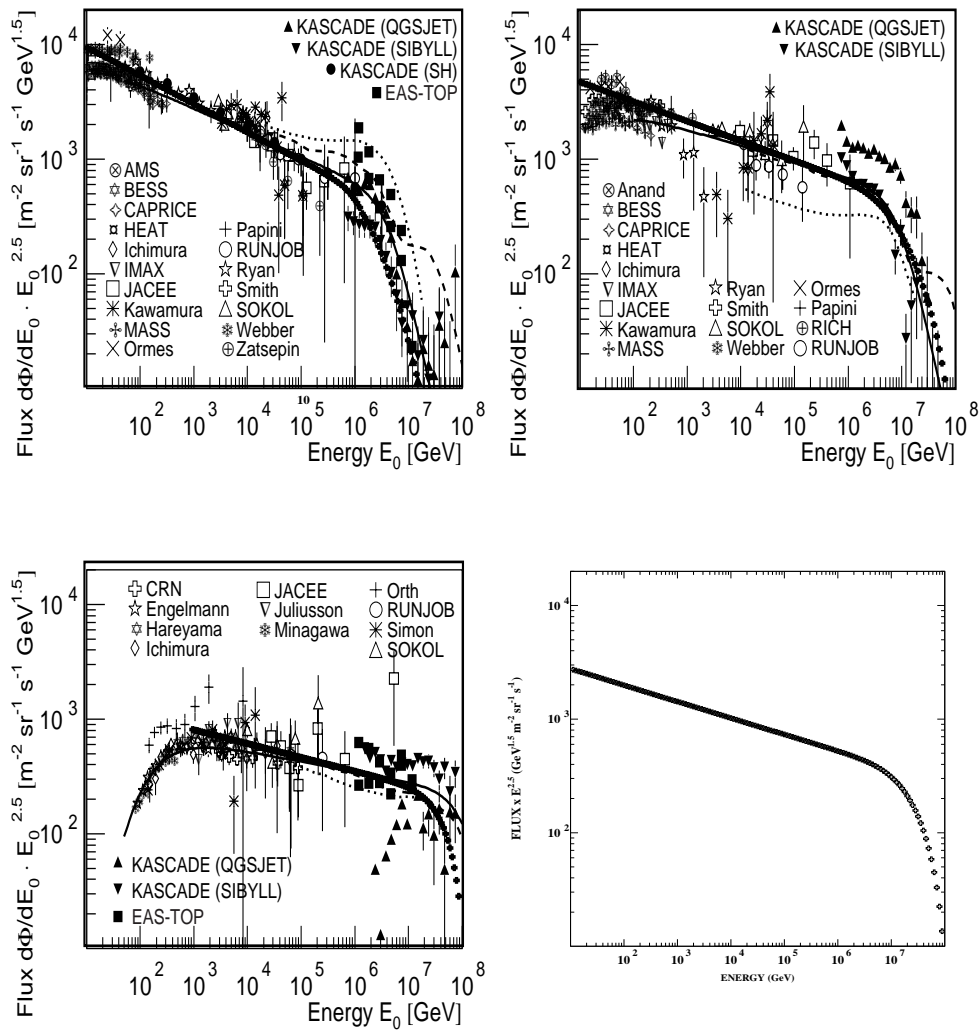


Figure 3: Comparison between the single-acceleration CB model predictions for the energy spectrum of various cosmic ray nuclei (thick line of crosses) and their energy spectrum as derived from various experiment and theoretical models and compiled by Hoerandel (2004). Top left – protons, top right – helium nuclei, bottom left – iron group nuclei and bottom right – CNO group nuclei.

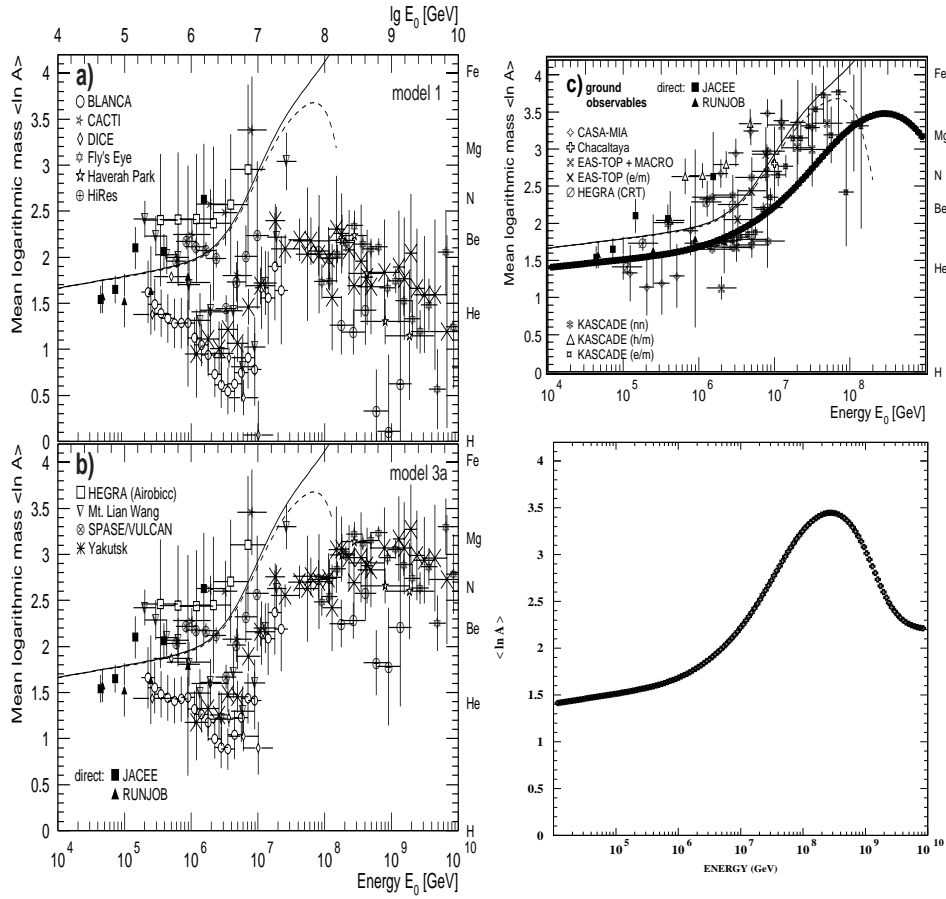


Figure 4: Comparison between the CB model prediction for the mean logarithmic atomic mass $\langle \ln A \rangle$ as function of CR energy (thick lines of crosses on the rhs) and $\langle \ln A \rangle$ as obtained by various experiments and compiled by Hoerandel 2004: (a) from measurements of the average depth of shower maximum interpreted with CORSIKA/QGSJET01, (b) interpreted with a modified version, and (c) from experiments measuring electrons, muons and hadrons at ground level.